

A Minimum SAR RF Pulse Design Approach for Parallel Tx with Local Hot Spot Suppression and Exact Fidelity Constraint

I. Graesslin¹, F. Schweser¹, B. Annighoefer¹, S. Biederer², U. Katscher¹, K. Nehrke¹, H. Stahl¹, H. Dingemans³, G. Mens³, and P. Börnert¹

¹Philips Research Europe, Hamburg, Germany, ²Institute of Medical Engineering, Lübeck University, Lübeck, Germany, ³Philips Medical Systems, Best, Netherlands

Introduction

With increasing field-strength, the local specific absorption rate (SAR) becomes a limiting factor for MR imaging applications. However, using parallel Tx systems, it becomes possible to tailor the E-fields in the RF pulse design. Certain SAR optimal algorithms have been proposed, e.g. [1], that constrain a specific local region for SAR (e.g., the eyes). This is in general insufficient for whole body imaging, as the location of SAR hot spots limiting the MR sequence is not fixed in the subject.

This paper presents 1. a method for SAR optimized RF pulse design following [2, 3, 4] and 2. a method for local hot spot reduction based on that technique. The concept was validated by simulations and experiments. The proposed method makes use of a graphics-processing unit (GPU)-based SAR calculation. It calculates the SAR according to [5] (almost) in real-time for a whole body bio-mesh.

Methods

For an N -channel Tx system, the excitation pattern can be written in matrix notation as $m=Ab$ [2], where m is an $M \times 1$ vector of the target excitation samples in the region of interest and b an $N \times 1$ vector of the RF samples containing T samples of the RF pulses $b_n, 1 \leq n \leq N$ of each coil. A is an $M \times NT$ matrix incorporating the B_1 map of each coil and the pre-defined k -space trajectory. Existing RF pulse design methods often optimize for low pulse peak power using, e.g., regularization techniques [2,4]. Other existing algorithms consider SAR at fixed regions [1, 3, 6, 7]. Provided that the RF field inside the subject responds linearly to the currents driving the field, the SAR can be expressed in a quadratic form in the pulse samples $b^\dagger Q b$, where † denotes the conjugate transpose and Q is a block-diagonal positive definite matrix resulting from the solution of Maxwell's equations and corresponding to a specific subject volume [6]. Zhu minimized the equation $b^\dagger Q b$ s.t. $m=Ab$ for Cartesian trajectories [6]. Then, the problem was generalized to arbitrary trajectories [2], and the solution (linear in m) was obtained by block-inversion $b = Dm$. In this study, the constraint was relaxed by minimizing $n^\dagger D^\dagger Q D n$ s.t. $\|m-n\|_2 = \epsilon$, solved with respect to n . Thus, to minimize SAR, small deviations ϵ from the demand pattern m are allowed, leading to a pattern n with small excitation errors, but potentially large SAR reduction. Now, $b=Dn$ represents the RF waveform, which exhibits a minimal energy dissipation and, simultaneously, an excitation error of ϵ . The combination of both problems gives insight into the role of the pattern design by making it possible to examine the impact of the excitation fidelity and analyze it with respect to critical geometrical structures. An advantage of the approach is that ϵ can be adjusted as a free parameter (i.e. is known a priori) for the pulse calculation. Via this mechanism, it is possible to explore the entire range of fidelity-SAR tradeoffs.

Based on the described (global) SAR minimization approach, a method for local hotspot reduction is proposed. This method introduces P new variables $\{q_i\}$ into the problem, which are the weighting factors specifying the trade-off between different hotspot regions. Depending on the spatial SAR distribution of an optimal RF pulse with respect to global SAR, hot spot reduction is introduced via $Q_i = Q_{global} + \sum q_i Q_{critical_region(i)}$. The problem reduces to finding the best weighting factors q_i to satisfy existing SAR limits and to decrease the limiting local SAR value most. To this aim, E-fields were calculated for an ideally decoupled 3T 8-channel body coil [8], according to [9]. A bio-mesh (Philips Medical Systems, Cleveland) of the "Visible Human Male" with about 750k cells was used. The pre-calculated E-fields were averaged according to [10], and the SAR calculation was implemented on a high performance graphics card (Quadro FX 5600, NVIDIA® Corporation, USA) with 128 processors (3.8ms/sample). The 2D Transmit SENSE RF pulses [4] were calculated using the above described algorithm with a calculation time between 4 to 9 sec. on a PC with Intel™ Xeon 5140 @ 2.33GHz (32x32 FOX, R=4). A comparison was made with an algorithm without RMS control and SAR optimization [11]. Spiral k -space trajectories were used with a numerical field-of-excitation of 32×32 pixels as well as with reduction factors R up to 7. Bloch simulations were carried out using 32×32 pixels. Experiments were performed on a whole body 3T MRI system (Achieva, Philips Medical Systems, The Netherlands) extended to eight parallel RF transmit channels [12]. In preparation of local excitation experiments of the kidneys, in vivo B_1 -maps using the AFI technique [13] were obtained separately for each transmit coil element (400 mm FOV, 64 scan matrix, $\alpha=75^\circ$, TR1=40ms, TR2=200ms).

Results and Discussion

Fig. 1 shows that the algorithm without SAR optimization leads to a significantly higher SAR compared with the SAR optimized method resulting in equal excitation and using the pattern modification, respectively. The SAR is decreasing with increasing RMS. Fig. 2 shows the results of simulations for two different patterns (local excitation of the kidney and liver) for R up to 7. For all cases, the SAR optimized algorithm outperforms the algorithm without SAR optimization. However, the improvement becomes smaller with increasing R , as the degrees of freedom decreases that can be deployed for SAR reduction. Fig. 3a) shows an image of the abdominal region, with the kidneys highlighted in red. Fig. 3b) shows the local excitation pattern of the kidneys, and Fig. 3c) depicts the experimental verification. Fig. 4 shows the results of the local SAR hotspot suppression for the pelvic region. The limiting hotspot in Fig. 4a) was reduced by 47% (Fig. 4b)) while meeting the SAR limits in all other regions according to [5]. It is worth mentioning that the potential of local SAR hot spot suppression highly depends on the excitation pattern, the reduction factor, the patient model, and its position within the coil.

By enabling a simple Minimum Norm Design analysis [14] the described approach can also be formulated in k -space similar to [4].

Conclusion

An RF pulse design technique was presented, which combines several advantages of existing algorithms. A precise control of the excitation fidelity up to zero residual error is possible. This allows for the analysis of the impact of the pattern modification on SAR and the determination of the best trade-off between SAR and residual error. Based on this approach, a method for local SAR hotspot suppression was demonstrated, which is very important for SAR limited scans, e.g. Transmit SENSE with high reduction factors at high field strength.

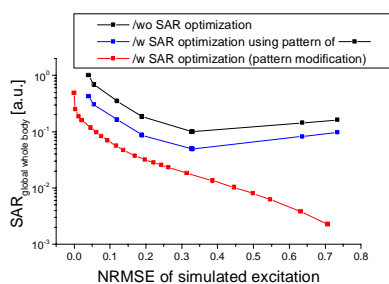


Fig. 1: SAR comparison of the different algorithms for various normalized RMS errors (NRMSE) for kidney excitation ($R=4$).

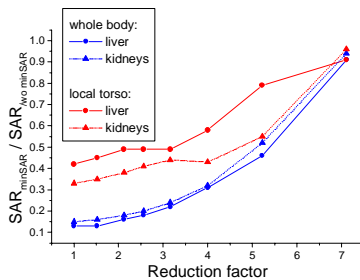


Fig. 2: SAR ratio of the different algorithms for kidney/liver excitation for global whole body and local torso SAR.

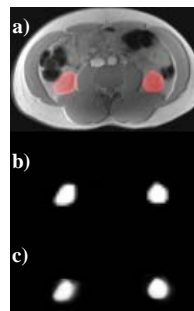


Fig. 3: a) Abdominal region, b) excit. pattern of kidneys, c) phantom experiment.

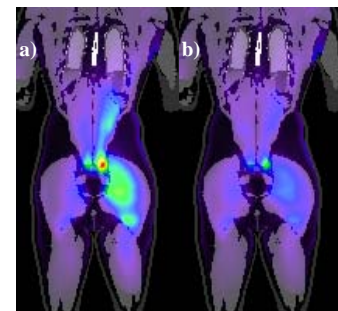


Fig. 4: Hotspot in the pelvic region a) without and b) with local hotspot reduction.

References

- [1] Brunner DO, et al. [2007] ISMRM 15:1690
- [2] Grissom W, et al. [2006] ISMRM 14:3015
- [3] Zhu Y [2006] ISMRM 14:599
- [4] Katscher U, et al. [2003] MRM 49:144-150
- [5] IEC [2002] 60601-2-33, 2nd Ed.
- [6] Zhu Y [2004] MRM 51:775-784
- [7] Zelinski AC, et al. [2007] ISMRM 15:1699
- [8] Vernickel P, et al. [2007] MRM 58(2):381-9
- [9] Graesslin I, et al. [2007] ISMRM 15:1090
- [10] IEEE Inc. [2002] Std C95, 3rd Ed.
- [11] Graesslin I, et al. [2007] ISMRM 15:1086
- [12] Graesslin I, et al. [2006] ISMRM 14:129
- [13] Yarmykh VL MRM [2007] 57(1):192-200
- [14] Wiesinger F, et al. [2007] ISMRM 15:678